HHS Public Access

Author manuscript

Hum Mutat. Author manuscript; available in PMC 2016 March 01.

Published in final edited form as:

Hum Mutat. 2015 March ; 36(3): 369–378. doi:10.1002/humu.22754.

Heterozygous triplication of upstream regulatory sequences leads to dysregulation of matrix metalloproteinase 19 (*MMP19*) in patients with cavitary optic disc anomaly (CODA)

Ralph J. Hazlewood[1,2], **Benjamin R. Roos**[1,2], **Frances Solivan-Timpe**[1,2], **Robert A. Honkanen**[3], **Lee M. Jampol**[4], **Stephen C. Gieser**[5], **Kacie J. Meyer**[1,2], **Robert F. Mullins**[1,2], **Markus H. Kuehn**[1,2], **Todd E. Scheetz**[1,2], **Young H. Kwon**[1,2], **Wallace L.M. Alward**[1,2], **Edwin M. Stone**[1,2,6], and **John H. Fingert**[1,2,*]

[1]Department of Ophthalmology and Visual Sciences, Carver College of Medicine, University of Iowa, Iowa City, IA 52242 USA

[2]Stephen A. Wynn Institute for Vision Research, University of Iowa, Iowa City, IA 52242 USA

[3]Department of Ophthalmology, State University of New York at Stony Brook, Stony Brook, New York 11733 USA

[4]Department of Ophthalmology, Feinberg School of Medicine, Northwestern University, Chicago, Illinois 60611 USA

[5]Wheaton Eye Clinic, Wheaton, IL 60187 USA

[6]Howard Hughes Medical Institute, Iowa City, IA 52242 USA

Abstract

Patients with a congenital optic nerve disease, cavitary optic disc anomaly (CODA), are born with profound excavation of the optic nerve resembling glaucoma. We previously mapped the gene that causes autosomal dominant CODA in a large pedigree to a chromosome 12q locus. Using comparative genomic hybridization and quantitative PCR analysis of this pedigree, we report identifying a 6Kbp heterozygous triplication upstream of the matrix metalloproteinase 19 (*MMP19*) gene, present in all 17 affected family members and no normal members. Moreover, the triplication was not detected in 78 control subjects or in the Database of Genomic Variants. We further detected the same 6Kbp triplication in 1 of 24 unrelated CODA patients and in none of 172 glaucoma patients. Analysis with a luciferase assay showed that the 6Kbp sequence has transcription enhancer activity. A 773bp fragment of the 6Kbp DNA segment increased downstream gene expression 8-fold, suggesting that triplication of this sequence may lead to dysregulation of the downstream gene, *MMP19*, in CODA patients. Lastly, immunohistochemical analysis of human donor eyes revealed strong expression of MMP19 in optic nerve head. These data strongly suggest that triplication of an enhancer may lead to overexpression of MMP19 in the optic nerve which causes CODA.

[*]To whom correspondence should be addressed: John H. Fingert MD PHD, Department of Ophthalmology and Visual Sciences, Carver College of Medicine, University of Iowa, 3111B MERF, 375 Newton Road, Iowa City, IA 52242, USA. Tel: +1 3193357508, Fax: +1 8774349041, john-fingert@uiowa.edu.

Keywords

Glaucoma; MMP19; CODA; copy number variation; cavitary optic disc anomaly; coloboma; reporter assay; immunohistochemistry; qPCR; functional assay

INTRODUCTION

The optic nerve (cranial nerve II) conveys visual signals from the retina to the brain. The inner most cells of the retina, the retinal ganglion cells, project axons that converge to form the optic nerve as they exit the eye en route to the brain. Diseases of the optic nerve may be recognized and categorized in part by characteristic changes to the appearance of the optic nerve head that are visible during an eye examination. One group of optic nerve diseases (the glaucomas) is defined largely by progressive loss of optic nerve fibers and the resulting excavated or cupped contour of the optic nerve head. Glaucoma typically has an onset later in life and affects up to 60 million adults worldwide (Roodhooft 2002; Quigley and Broman 2006). A spectrum of congenital malformations of the eye (optic nerve coloboma, megalopapilla, optic pit, and morning glory disc anomaly) also have an excavated optic nerve head (Brodsky 1994) that resembles the nerve appearance in glaucoma. Some syndromic cases of optic nerve head malformations have been associated with mutations in *PAX2* (OMIM 167409) (Dureau et al. 2001) or *PAX6* (OMIM 607108) (Azuma et al. 2003). Optic nerve colobomas and renal disease may be caused by mutations in the *PAX2* gene (Dureau et al. 2001), while other sporadic cases of optic nerve disease have been attributed to *PAX6* mutations (Azuma et al. 2003). Finally, rare families have been reported with autosomal dominant inheritance of congenitally excavated optic nerves as well as other features of optic pit, optic nerve coloboma, and morning glory disc anomaly, which has been termed cavitary optic disc anomaly (CODA) (Savell and Cook 1976; Slusher et al. 1989; Honkanen et al. 2007).

Clinical similarities between CODA and normal tension glaucoma, glaucoma that occurs without elevated intraocular pressure, have suggested that these conditions may have overlapping pathophysiology. Both conditions have similar appearing optic nerves that have an excavated topography and both conditions develop without elevated intraocular pressure. In some cases, patients with CODA have had progressive worsening of optic nerve excavation, which is a hallmark of glaucoma (Moore et al. 2000; Honkanen et al. 2007). However, there are some clear differences between CODA and glaucoma. Patients with CODA have a strong predilection for retinal detachments and/or separation of the retinal layers (retinoschisis) that lead to profound central vision loss, while such retinal abnormalities are less commonly seen in glaucoma patients with large optic cups and no signs of congenital optic pits (Spaide et al. 2003) (Hollander et al. 2005) (Kahook et al. 2007) (Zumbro et al. 2007). More than half of patients with CODA develop retinal detachments and/or retinoschisis in one or both eyes (Honkanen et al. 2007). The same genetic defect that causes CODA also greatly increases risk for retinal disease.

We previously mapped the disease-causing gene for familial autosomal dominant CODA to a novel genetic locus on chromosome 12q with linkage analysis of a large autosomal

dominant pedigree (Fingert et al. 2007). This CODA locus spans 13.5 Mbp and more than 200 genes. Members of the pedigree were initially sequenced for disease-causing mutations in three candidate genes (*GDF-11*, *WIF1*, and *NEUROD4*) within the locus, but no variations were detected (Fingert et al. 2007). Here we report additional studies to identify and characterize the mutation in the chromosome 12q locus that causes CODA in our large pedigree using DNA sequencing, copy number variation (CNV) analysis, immunohistochemistry, and a reporter gene assay to assess mutation effects on transcription.

MATERIALS AND METHODS

Study sample subjects and controls

Seventeen clinically affected family members and one obligate carrier for CODA in a large pedigree (Supp. Figure 1A) were previously described (Fingert et al. 2007; Honkanen et al. 2007). Patients received complete ophthalmic examinations by one of the authors (L.M.J., W.L.M.A., or R.A.H.) or fellowship trained glaucoma-specialists. Affected family members have cavitary optic disc anomalies with clinical criteria previously described (Fingert et al. 2007; Honkanen et al. 2007). Additional CODA patients (Supp. Figure 1B), patients with glaucoma, and matched control subjects were recruited from the clinics at the University of Iowa using previously described criteria (Fingert et al. 2011). Informed consent was obtained for study participants and was conducted with the approval of the University of Iowa's Institutional Review Board. DNA was prepared from blood samples from each study participant as previously described (Buffone and Darlington 1985).

Candidate gene screening and exome sequencing

Testing candidate genes for disease-causing mutations was facilitated with the TrAPSS software program, which prioritized gene segments for sequencing based on annotation and homology (O'Leary et al. 2007). Candidate genes in the CODA locus were PCR amplified and analyzed for mutations by single stranded conformation polymorphism (SSCP), high resolution melt (HRM) analysis and/or bi-directional sequencing as previously described (Fingert et al. 1999; Fingert et al. 2011). Primer sequences are available upon request.

One family member with CODA (Patient IV-8, Supp. Figure 1A) was additionally tested for disease-causing mutations by conducting whole exome sequencing and restricting our analysis to the variants lying within the linked chromosome 12q locus. Exome capture was conducted using SureSelect Human All Exon v2 (Agilent, Santa Clara, CA) using the manufacturer's protocol and paired-end, 50 nucleotide reads were obtained using a HiSeq2000 (Illumina, San Diego, CA) which achieved an average exon coverage of 65X. Identified sequence variants were filtered to include only those variants located within the chromosome 12 CODA locus (defined by genetic markers D12S1618 and D12S1702), non-synonymous coding sequence variants, and variants that occurred at a frequency of less than 1% in 1000 genomes and less than 0.6% in the Exome Sequence Project public databases (1000 Genomes Project Consortium et al. 2012; EVS).

CNV analysis, array CGH, and quantitative PCR

Family members of Pedigree IP-09-47 and 981-R were genotyped with a custom Sureprint G3 8×60K Human CGH microarray (Sureselect, Agilent, CA USA). The genomic interval (NCBI37/hg19) chr12:53,586,000-58,865,000 was assayed with approximately 100bp probe spacing and processed according to the manufacturer's protocol. Array CGH was performed using 0.5μg of patient DNA and 0.5μg of human reference DNA (Promega, WI). Patient genomic DNA and reference DNA from normal control were labeled in parallel, each with a distinct fluorescently labeled probe and co-hybridized to the array. Data was analyzed using Agilent CytoGenomics v2.7 software.

TaqMan Copy Number Assays were used in real time quantitative PCR (qPCR) done in triplicate and analyzed with Copy Caller Software v1.0 (Applied Biosystems, CA) in accordance to manufacturer's conditions and protocols. The coordinates for the TaqMan probes used are shown in Supp Table S1. Detected and confirmed variants were submitted to ClinVar (http://www.ncbi.nlm.nih.gov/clinvar/).

Cloning and Promoter constructs

The triplicated 6 Kbp upstream sequence of *MMP19* (RefSeq NM_002429.4) was PCR amplified from RPCI11-559I11 BAC clone (Empire Genomics, NY) and cloned into TOPO-XL shuttle vector (Invitrogen, CA). The CNV DNA sequence in TOPO-XL vector was then digested with *KpnI* and *XhoI* and cloned upstream of the Luciferase gene into the pGL3-Promoter vector (Promega, WI, USA, Supp. Figure 2) to generate the vector now called “pGL3 (Full Length 6Kb Fragment)”. The pGL3-Promoter vector contains the SV40 promoter but no enhancer element. Clones were bi-directionally sequenced to confirm orientation, size and validate sequence. Seven subclones of the 6 Kb fragment, each less than 1 Kbp in size were generated from the Full Length vector by PCR with overlapping primer pairs using the same restriction digestions enzymes *KpnI* and *XhoI*. These smaller fragments were then subcloned into pGL3-Promoter vectors. These constructs were listed as pGL3-ProA, pGL3-ProB, pGL3-ProC, pGL3-ProD, pGL3-ProE, pGL3-ProF, and pGL3-ProG (Figure 1A). Primer sequences are available upon request.

Cell culture and transient transfection with luciferase assays

Luciferase transfection assays were performed in HEK293T cells. Cells were maintained in Dulbecco's Modified Eagle's medium supplemented with 10% fetal bovine serum. Low passage cells were plated onto 6-well tissue culture plates (Corning, NY, USA) at a density of 500,000 cells/well until 70-90% confluent. Cells were transfected in triplicate with 2.5μg of pGL3 (Full Length 6Kb Fragment) plasmid and 200ng of CMV-*Renilla* plasmid and permeated with 8μl Lipofectamine 2000 reagent (Invitrogen, CA, USA). Co-transfection with *Renilla* served as an internal control to assess transfection efficiencies. DNA and Lipofectamine complexes were added to each well and incubated for 24 hours at 37°C in a CO^2 incubator. Following incubation, cells were lysed and Luciferase activity measured using Dual-Glo Luciferase assay system (Promega, WI, USA). Luminescence was recorded using NOVOstar microplate reader (BMG LABTECH, Germany). Firefly Luciferase activity for each DNA fragment was normalized to empty vector and relative Luciferase activity was calculated. Data is shown as fold change compared to empty vector control,

pGL3 (Control Promoter). All experiments were repeated at least three times and statistical significance calculated with one-way ANOVA and two-tailed Student's t test.

Immunohistochemistry

Human donor eyes were obtained from the Iowa Lions Eye Bank following informed consent from the donor's families. Human donor eyes without eye disease were fixed with 4% paraformaldehyde in phosphate buffered solution (PBS) within 8 hours of death. Wedges of retina and optic nerve were cryopreserved in sucrose solution and embedded in optimal cutting temperature solution (Barthel and Raymond 1990). Polyclonal antibodies directed against MMP19 (1:100, ab2 AV32315; Sigma Aldrich, St. Louis, MO, USA) were used as previously described (Fingert et al. 2011). Co-labeling experiments were performed using anti-MMP19 and a polyclonal antibody against glial fibrillary acidic protein (GFAP 1:100, SAB2500462; Sigma Aldrich, St. Louis, MO USA). Briefly, cryostat sections were collected, prepared, and blocked in 1% BSA/0.1% Triton X-100 for 15 minutes followed by incubation with anti-MMP19 overnight at 4°C. For co-labeling experiments, sections were incubated with anti-MMP19 and anti-GFAP overnight at 4°C. Following primary incubation with anti-MMP19 and anti-GFAP, sections were washed in 3× 5 minute washes in PBS, and then incubated with Alexa-488 conjugated donkey anti-rabbit and Alexa-546 conjugated donkey anti-goat secondary antibodies (1:200, Invitrogen, CA, USA) and 4’6-diamidino-2-phenylindole (DAPI) for 30 minutes. Sections were washed again 3 times for 15 minutes, mounted in Aqua-Mount (Thermo Scientific MI, USA), and observed under fluorescence microscopy.

RESULTS

In our previous reports we described the clinical features of CODA in 17 members of a five-generation pedigree with autosomal dominant inheritance of disease (Pedigree 981-R, Supp. Figure S1A) (Moore et al. 2000; Fingert et al. 2007; Honkanen et al. 2007). Linkage analysis of this family mapped the mutation that causes CODA to a 13.47 Mbp segment of chromosome 12q between genetic markers D12S1618 (53,892,649) bp and D12S1702 (67,359,260 bp) (Fingert et al. 2007).

Candidate gene screening

We previously tested members of pedigree 981-R for CODA-causing mutations in the entire coding sequence of three genes in the linked chromosome 12q14 locus (*GDF-11, WIF1*, and *NEUROD4*), however, none were detected (Fingert et al. 2007). We selected additional candidate genes in the linked region with known gene function and/or ocular expression that are consistent with a role in CODA pathogenesis (i.e. function in neurogenesis and expression in the optic nerve or retina). DNA from two members of pedigree 981-R (Supp. Figure S1A, III-10 and IV-8) was tested for CODA-causing mutations by sequencing the entire coding sequence of seven additional candidate genes (TBK1, SILV, ZNF1A4, ADMR, STAC3, BLOC1S1, and SLC6A7). Functional domains and conserved sequences were identified in an additional 47 candidate genes (Supp. Table S2) using the TrAPSS software package (O'Leary et al. 2007). Using a combination of single strand conformation polymorphism (SSCP), high-resolution melt (HRM) analysis, and bi-directional Sanger

sequencing, these high interest gene segments were also tested for CODA-causing mutations. Several non-synonymous sequence variations were detected in these candidate genes, but no plausible coding sequence mutations were found that are both co-inherited with disease in pedigree 981-R and absent from control subjects (data not shown). We subsequently used whole exome sequence analysis of one CODA patient in pedigree 981-R (Patient IV-8, Supp. Figure S1A) as a more comprehensive search for disease-causing mutations within the chromosome 12q locus. Two rare heterozygous, non-synonymous coding sequence variants were detected, missense mutation R464Q in *ITGA5* and frame-shift mutation c110-111insA in *CD63*. However, when the entire 981-R pedigree was tested with Sanger sequencing, the R464Q variant in *ITGA5* was not co-inherited with disease, ruling it out as a potential cause of CODA. The presence of the other variant detected by exome sequencing, the *CD63* frame-shift mutation, could not be confirmed with Sanger sequencing, suggesting that its initial discovery was an exome sequencing error. Overall, the analysis of the exome data did not identify any plausible disease-causing variants in genes within the linked chromosome 12q locus.

Copy number variation (CNV) analysis

We also tested CODA pedigree 981-R (Supp. Figure S1A) for the presence of CNVs within the linked chromosome 12q locus. DNA from 2 affected members of CODA pedigree 981-R (Supp Figure S1A, III-10 and IV-8) was genotyped for CNVs in a comparative genomic hybridization (CGH) experiment using a custom chromosome 12 Agilent CGH array with 60,000 probes distributed across the chromosome 12q locus according to the manufacturer's protocol. CNVs in this region of chromosome 12q have been previously detected spanning the normal tension glaucoma gene, TANK binding kinase 1 (*TBK1*) (Fingert et al. 2011; Kawase et al. 2012; Awadalla et al. 2014; Ritch et al.), however no *TBK1* duplications or deletions were identified in DNA samples from our CODA patients. Both CODA patients were found to carry 2 extra copies (4X) of a 6 Kbp DNA segment, chr12:g. 56238827_56244961 (3), within the CODA locus and 2.1 Kbp upstream of the matrix metalloproteinase 19 (*MMP19* OMIM 601807) gene (Figure 1A). The presence of the CNV was further confirmed with a TaqMan quantitative PCR (qPCR) assay. When the entire pedigree was tested with the qPCR assay, we discovered that this CNV is co-inherited with CODA in all 17 affected family members and absent from unaffected members. The autosomal dominant inheritance pattern of the 4X CNV indicates that it is a heterozygous 6 Kbp triplication. Also, this triplication was not detected in 78 normal control subjects (Figure 2), nor was it previously reported in the online Database of Genomic Variants (http://dgv.tcag.ca/dgv/app/home).

An additional 24 unrelated patients with a clinical diagnosis of CODA or its component features (optic pit, optic nerve coloboma, or morning glory disc anomaly) were tested for evidence of a CNV upstream of *MMP19* using our qPCR assay. One of these 24 patients was found to have a DNA triplication upstream of *MMP19*, which suggests that *MMP19* CNVs may contribute some fraction of additional cases of CODA. This patient (Supp Figure S1B, Pedigree IP-09-47, patient III-1) is a member of a three-generation pedigree with two other family members affected with CODA including his mother and maternal grandmother. Testing DNA from his affected mother (Supp. Figure S1B, Pedigree IP-09-47, II-1) with our

qPCR assay showed that she also carries a triplicated DNA sequence upstream of *MMP19*. DNA was not available from the patient's maternal grandmother (Supp Figure S1B, Pedigree IP-09-47, I-2). Analysis of IP-09-47 family members with a custom Agilent CNV microarray identified a 6 Kbp triplication with the same borders as the CNV detected in pedigree 981-R (Figure 1A).

CNVs with the same borders were detected in two CODA pedigrees (981R and IP-09-47) that are not known to be genealogically related. Consequently, we investigated the possibility that the CNVs in each family arose independently on different chromosome 12q haplotypes by genotyping both families at genetic markers flanking the CNVs. Single nucleotide polymorphism (SNP) markers and short tandem repeat polymorphism (STRP) markers closely flanking the CNV were typed in both families (Supp. Table S3). Allele sharing was observed between the two pedigrees at markers most closely flanking the CNV. These data do not provide evidence to suggest the CNVs in pedigree 981-R and IP-09-47 arose independently. However, the power of this analysis was limited by the informativity of the flanking markers and by the small size of pedigree IP-09-47.

Finally, the entire coding sequence of 13 of our cohort of 24 unrelated CODA patients was evaluated for mutations. A synonymous Val176Val change was detected in one individual with CODA and no non-synonymous changes were detected.

Overall, these data show that a CNV upstream of *MMP19* is associated with CODA. We further explored the DNA sequence spanned by this CNV for a role in CODA pathogenesis by testing a cohort of patients for mutations. Our cohort of 24 unrelated CODA patients was tested for mutations in the 6 Kbp region upstream of *MMP19* that was encompassed by the CNV. Approximately 71% of this region was tested for mutations using unidirectional Sanger sequencing, while 29% of the region was composed of highly repetitive sequences and could not be assessed reliably with this method. Five variations were detected (Supp Table S4), however, four of these variants were judged to be implausible causes of CODA due to their relatively high frequency in 1000 Genomes Project (Genomes Project, et al., 2012) and control subjects. The fifth variant, which was detected in a single CODA patient and was absent from control populations, has unknown significance. These data suggest that currently detectable DNA sequence variations within the 6kb region upstream of *MMP19* are unlikely to be common causes of CODA. Additionally, no obvious difference in optic nerve appearance was noted between those CODA subjects found to carry the *MMP19* CNV and those without the CNV.

One mechanism for the generation of CNVs is non-allelic homologous recombination due to the presence of repetitive DNA sequences. Consequently, we analyzed DNA sequence upstream of *MMP19* in search of repetitive sequences that might have been involved with the development of the CNV in our CODA patients. We identified numerous *Alu* elements that are members of the short interspersed elements (SINE) family of repetitive sequences upstream of the *MMP19* (Figure 1B). A high density of *Alu* elements are located on either side of the 6 Kbp DNA sequence that is triplicated in patients with CODA in pedigrees 981-R and IP-09-47. Further sequence analysis showed that this 6 Kbp sequence spans a region of DNAseI hypersensitivity and H3K27 acetylation sites that are often found near regulatory

sequences (Figure 1C). The positions of several potential binding sites for transcription factors are also clustered on this region upstream of *MMP19* (Figure 1C).

Testing glaucoma patients for the chromosome 12q CNV

The chief feature of CODA is an excavated optic nerve head that resembles damage caused by glaucoma. Consequently, we tested cohorts of patients with primary open angle glaucoma that occurs at normal intraocular pressure (n = 84) or at elevated intraocular pressure (n = 88) to see if a similar genetic defect might be involved in the pathogenesis of glaucoma. These 172 glaucoma patients were tested for CNVs using our qPCR assay, however, none were detected.

Transcription activity of the chromosome 12q14 CNV

The location of the 6 Kbp triplication, which is 2.1 Kbp upstream of *MMP19*, suggests that it might contain transcription regulatory elements that alter gene expression. Consequently, this DNA sequence was investigated for transcriptional activity using a luciferase reporter gene assay. A single copy of the 6 Kbp DNA sequence spanned by the CNV was transfected upstream of the luciferase gene in a vector with a control SV40 promoter (pGL3, Promega) (Supp. Figure S2). The transcriptional activity of this DNA segment was measured in HEK293T cells 24 hours after transfection. Cells transfected with this DNA segment produced a 1.3-fold increase in luciferase activity compared with cells transfected with pGL3 vector containing no enhancer sequences (Figure 3A). Large DNA sequence such as the 6 Kbp CNV identified in this study may harbor multiple enhancer and/or silencer elements and motifs (Kleinjan, et al., 2008; Ochi, et al., 2012; Sanyal, et al., 2012). In order to fine map the location of individual enhancer elements, the DNA segment spanned by the CNV was subcloned into 7 smaller overlapping fragments pGL3-ProA, pGL3-ProB, pGL3-ProC, pGL3-ProD, pGL3-ProE, pGL3-ProF, and pGL3-ProG (Figure 1A) and transfected into HEK293T cells. Cells transfected with the vector containing DNA fragment pGL3-ProF produced the greatest luciferase activity. These cells generated 8-fold more luciferase activity than cells transfected with the vector containing no enhancer sequences, $p < 0.05$ (Figure 3B). Analysis of the pGL3-ProF DNA sequence with ENCODE data illustrated with UCSC Genome Browser (Rosenbloom, et al., 2012) identified DNaseI hypersensitivity sites and H3K27 acetylation marks, which are consistent with the presence of active regulatory elements (Jenuwein and Allis 2001; Berger 2002) in the DNA segment that is triplicated in our CODA patients. These data suggest that the CNV detected in CODA patients influences the expression of *MMP19* and the source of this enhancer activity is located within pGL3-ProF clone.

Immunohistochemistry

The localization of MMP19 within the human eye was investigated with immunohistochemistry using a polyclonal anti-MMP19 antibody. Given that the chief feature of CODA is a malformation of the optic nerve, we directed our analysis at the optic nerve and retina. The strongest immunoreactivity was detected in the head of the optic nerve (Figure 4A, D), with modest labeling in the neural retina.

MMP19 immunoreactivity was especially pronounced in the prelaminar region, laminar, and posterior lamina cribrosa region where there was punctate, but robust staining. Whereas some MMP19 immunolabeling was also observed at the transition between the posterior lamina cribrosa region and the retrolaminar region, this signal tapered off posteriorly, at the level at which axons become myelinated. In the retrolaminar optic nerve, some immunoreactivity was detected along the glial columns and ganglion cell axons.

To further characterize MMP19 in the optic nerve, we double-labeled tissue sections with anti-glial fibrillary acidic protein (GFAP), a marker for glial cells and astrocytes. We observed that MMP19 was highly localized in the optic nerve head (disc), whereas GFAP (Fig. 4) was detected in both the retina and optic nerve. These results demonstrate MMP19 expression at the site of injury, which is consistent with a role of MMP19 in the pathophysiology of CODA.

DISCUSSION

Using a range of detection techniques (CGH and qPCR), we have discovered a 6 Kbp heterozygous triplication upstream of *MMP19* in patients with CODA. This CNV is co-inherited with CODA and located within the chromosome 12q locus that was previously defined by our linkage studies of a large CODA pedigree (Pedigree 981-R, Supp. Figure S1A) (Fingert et al. 2007) and is absent from controls, unaffected family members, and the Database of Genomic Variants. To our knowledge, this is the first discovery of a CNV that is associated with the spectrum of congenital malformations of the optic disc, termed CODA. When we tested a panel of 24 unrelated individuals with CODA, we detected another individual with the same 6 Kbp CNV upstream of *MMP19*. Although this cohort of patients may be too small to determine the proportion of CODA that is caused by the *MMP19* gene with accuracy, these results do suggest that the CNV in our large pedigree is not an isolated case and that additional CODA patients may also have disease due to *MMP19* defects.

The appearance of the optic disc in patients with CODA and in patients with glaucoma is similar. CODA subjects have congenitally excavated discs and diminished visual fields. Furthermore, in some CODA patients, there is progressive excavation of the optic discs (Moore et al. 2000; Fingert et al. 2011), which is a core feature of glaucoma. These observations underscore the clinical overlap of CODA and glaucoma and suggest that CODA may be a valuable model to study the optic nerve disease in glaucoma. We explored this hypothesis by testing 172 glaucoma patients (84 with glaucoma that occurs at low intraocular pressure and 88 with glaucoma that occurs at high intraocular pressure) for the same *MMP19* CNV detected in our CODA pedigrees. Although we did not detect the 6 Kbp CNV upstream of *MMP19*, it remains possible that other *MMP19* promoter or coding sequence mutations are associated with glaucoma.

Our functional analyses of the *MMP19* gene have provided evidence that it has a role in the pathogenesis of CODA. First, our luciferase reporter gene studies have shown that the *MMP19* CNV contains an enhancer element that dysregulates expression of downstream genes (i.e. *MMP19*). Of note, these luciferase reporter experiments are in agreement with

previous reports that show *MMP19* mRNA expression is greatly increased in an animal model of glaucoma (DBA/2J mice) (Howell et al. 2011). Second, our expression studies have shown that MMP19 is most highly expressed in the optic nerve head, the tissues of the eye most affected by CODA. The strong expression of MMP19 in human optic nerve (Figure 4) makes dysregulation of *MMP19* a biologically plausible cause of the optic nerve malformations in CODA subjects. However, additional studies (i.e. recapitulating the CODA phenotype with transgenic *MMP19* animals) will be needed to provide the ultimate proof that dysregulation of *MMP19* expression causes optic nerve excavation in CODA.

Although our studies have identified an enhancer mutation that may be an important regulator of *MMP19* expression in CODA patients, many other factors influence expression of MMP genes. Transcription factors such as AP-1 (Fini et al. 1994), TGF-B (Fini et al. 1995), and Pax-6 (Sivak and Fini 2002) are known to regulate MMP transcription. Mutations in MMP promoter sequences that influence transcription have also been reported (Sternlicht and Werb 2001). Similarly, factors in the microenvironment are known to influence MMP expression, including extracellular matrix proteins (Sternlicht and Werb 2001); cytokines and growth factors (Fini et al.); and molecules that alter cell shape (Kheradmand et al. 1998). MMP19 proteinase activity is also highly regulated by processes that control its secretion and activation and by endogenous tissue inhibitors of matrix metalloproteinases (TIMPs) (Sternlicht and Werb 2001; Egeblad and Werb 2002). Each of these factors may also contribute to regulation of MMP19 expression and activity in health and in disease (i.e. CODA).

Model of MMP19 and CODA

The known function of matrix metalloproteinases (MMPs) is consistent with our hypothesis that increased MMP19 activity causes CODA. MMPs are tightly-regulated extracellular zinc-binding endoproteases that maintain and degrade basement membranes and all types of extracellular matrix components and tissue architecture. These properties make MMPs attractive candidates for altering the structure of the optic nerve head and causing CODA. Moreover, defects in other MMPs have already been associated with primary angle closure glaucoma in humans (Wang et al. 2006; Cong et al. 2009) and open angle glaucoma in beagles (Kuchtey et al. 2011).

The optic nerve head is composed primarily of axons projecting from the retinal ganglion cells and glial cells (astrocytes). The axons are supported by a collagenous structure, the lamina cribrosa, as they pass through the scleral canal and exit the posterior of the eye en route to the lateral geniculate nucleus of the thalamus and the vision centers of the cortex (Figure 5A). In our model, we hypothesize that increased MMP19 enzymatic activity in the optic nerve head may undermine the insertion of the lamina cribrosa and lead to a collapse of this support structure and malformation of the optic nerve head that is characteristic of CODA (Figure 5B). Prior investigations of the biological processes that lead to cupping in experimental models of glaucoma in non-human primates have also suggested that proteinase activity may be important in alterations of the lamina cribrosa and optic disc cupping (Agapova et al. 2003; Roberts et al. 2009; Downs et al. 2011; Hernandez 2013).

MMP19 and retinal disease of CODA

Patients that are born with CODA frequently develop retinal disease later in life. More than half of patients with CODA have retinal detachments and/or retinoschisis (Postel et al. 1998; Honkanen et al. 2007). The nature of these acquired retinal abnormalities and their cause has not been definitively established, however, several hypotheses have been advanced. Some reports suggest that subtle breaks in the membrane that overlies the optic disc in CODA patients allows fluid to enter the subretinal space and cause retinoschisis and/or retinal detachment (Postel et al. 1998). Other studies have suggested that malformation of the optic disc allows an abnormal communication between the sub-arachnoid and sub-retinal spaces that allows cerebrospinal fluid to collect within the retina and produce retinoschisis and/or retinal detachments (Krivoy et al. 1996). Finally, some data suggests that CODA patients develop retinoschisis as a primary defect (Lincoff et al. 1993; Lincoff et al. 1996).

Our research suggests that the same *MMP19* mutation that causes optic nerve head malformation may also be a primary cause of acquired retinal abnormalities in CODA patients. Although our immunolabeling experiments showed strongest expression of MMP19 in the optic nerve head, we also observed weak labeling in the retina (Figure 4 and data not shown). MMPs modulate the normal interactions between retinal cells and the extracellular matrix that are necessary for cell adhesion, cell proliferation, and retinal architecture (Li and Sakaguchi 2002). Consequently, abnormal increases of MMP19 expression due to the enhancer mutation might disrupt cell adhesion and retinal architecture and cause a delamination of the retina resulting in retinoschisis and/or retinal detachment. These data suggest that mutation of *MMP19* may cause both the optic nerve malformation and retinal abnormalities that are hallmarks of CODA.

Analysis of the DNA sequence upstream of *MMP19* has provided key insights into the mechanism that caused the CNV in our CODA patients. This CNV is surrounded by repetitive DNA sequences, *Alu* elements (Figure 1B), which suggests that this triplicated DNA sequence was likely generated by non-allelic homologous recombination. *Alu*-mediated recombination errors and *Alu* element insertions have been previously reported as causes of several other ocular diseases including ocular albinism (Schiaffino et al. 1995), retinoschisis (Huopaniemi et al. 2000), dominant optic atrophy (Gallus et al. 2010), and retinitis pigmentosa (Abu-Safieh et al. 2006; Mackay et al. 2010; Tucker et al. 2011). The discovery of an *Alu*-mediated CNV in CODA patients further indicates the important role these repetitive elements may have in the pathogenesis of ophthalmic diseases. To our knowledge, this finding represents the first evidence that dysregulation of genes involved in extracellular matrix turnover is the primary cause of optic nerve and retinal disease seen in CODA patients. Although we did not detect the same *MMP19* CNV in patients with glaucoma, it is still possible that abnormal MMP19 function (due to different *MMP19* gene defects, aberrant transcriptional regulation, or environmental influences) may have a role in the pathophysiology of cupping. Future studies of *MMP19* gene regulation in CODA and in glaucoma may provide new insights into mechanisms of optic nerve excavation or cupping that is the chief sign of these important vision threatening optic nerve diseases.

Supplementary Material

Refer to Web version on PubMed Central for supplementary material.

Acknowledgments

Grant Sponsors: This work was supported in part by NIH (R21 EY24621, R01EY018825, R01EY023512) to J.H.F.; the Lew R. Wasserman Award of Research to Prevent Blindness to W.L.M.A; the Dean's Graduate Fellowship, the University of Iowa to R.J.H.; NIH-sponsored Training grant to the Interdisciplinary Program in Genetics to R.J.H.; and Robert and Sharon Wilson.

REFERENCES

1000 Genomes Project Consortium. Abecasis GR, Auton A, Brooks LD, DePristo MA, Durbin RM, Handsaker RE, Kang HM, Marth GT, McVean GA. An integrated map of genetic variation from 1,092 human genomes. Nature. 2012; 491:56–65. [PubMed: 23128226]

Abu-Safieh L, Vithana EN, Mantel I, Holder GE, Pelosini L, Bird AC, Bhattacharya SS. A large deletion in the adRP gene PRPF31: evidence that haploinsufficiency is the cause of disease. Mol Vis. 2006; 12:384–388. [PubMed: 16636657]

Agapova OA, Kaufman PL, Lucarelli MJ, Gabelt BT, Hernandez MR. Differential expression of matrix metalloproteinases in monkey eyes with experimental glaucoma or optic nerve transection. Brain Res. 2003; 967:132–143. [PubMed: 12650974]

Awadalla MS, Fingert JH, Roos BE, Chen S, Holmes R, Graham SL, Chehade M, Galanopolous A, Ridge B, Souzeau E, Zhou T, Siggs OM, et al. Copy number variations of TBK1 in Australian patients with primary open angle glaucoma. Am J Ophthalmol. 2014

Azuma N, Yamaguchi Y, Handa H, Tadokoro K, Asaka A, Kawase E, Yamada M. Mutations of the PAX6 gene detected in patients with a variety of optic-nerve malformations. Am J Hum Genet. 2003; 72:1565–1570. [PubMed: 12721955]

Barthel LK, Raymond PA. Improved method for obtaining 3-microns cryosections for immunocytochemistry. J. Histochem. Cytochem. 1990; 38:1383–1388. [PubMed: 2201738]

Berger SL. Histone modifications in transcriptional regulation. Curr. Opin. Genet. Dev. 2002; 12:142–148. [PubMed: 11893486]

Brodsky MC. Congenital optic disk anomalies. Survey of Ophthalmology. 1994; 39:89–112. [PubMed: 7801227]

Buffone GJ, Darlington GJ. Isolation of DNA from biological specimens without extraction with phenol. Clin. Chem. 1985; 31:164–165. [PubMed: 3965205]

Cong Y, Guo X, Liu X, Cao D, Jia X, Xiao X, Li S, Fang S, Zhang Q. Association of the single nucleotide polymorphisms in the extracellular matrix metalloprotease-9 gene with PACG in southern China. Mol Vis. 2009; 15:1412–1417. [PubMed: 19633731]

Downs JC, Roberts MD, Sigal IA. Experimental Eye Research. Exp Eye Res. 2011; 93:133–140. [PubMed: 20708001]

Dureau P, Attie-Bitach T, Salomon R, Bettembourg O, Amiel J, Uteza Y, Dufier JL. Renal coloboma syndrome. Ophthalmology. 2001; 108:1912–1916. [PubMed: 11581073]

Egeblad M, Werb Z. New functions for the matrix metalloproteinases in cancer progression. Nat. Rev. Cancer. 2002; 2:161–174. [PubMed: 11990853]

Exome Variant Server, NHLBI GO Exome Sequencing Project (ESP). Seattle, WA: (URL: http://evs.gs.washington.edu/EVS/) [November 2014]

Fingert JH, Héon E, Liebmann JM, Yamamoto T, Craig JE, Rait J, Kawase K, Hoh ST, Buys YM, Dickinson J, Hockey RR, Williams-Lyn D, et al. Analysis of myocilin mutations in 1703 glaucoma patients from five different populations. Hum Mol Genet. 1999; 8:899–905. [PubMed: 10196380]

Fingert JH, Honkanen RA, Shankar SP, Affatigato LM, Ehlinger MA, Moore MD, Jampol LM, Sheffield VC, Stone EM, Alward WLM. Familial cavitary optic disk anomalies: identification of a novel genetic locus. Am J Ophthalmol. 2007; 143:795–800. [PubMed: 17368552]

Fingert JH, Robin AL, Stone JL, Roos BR, Davis LK, Scheetz TE, Bennett SR, Wassink TH, Kwon YH, Alward WLM, Mullins RF, Sheffield VC, et al. Copy number variations on chromosome 12q14 in patients with normal tension glaucoma. Hum Mol Genet. 2011; 20:2482–2494. [PubMed: 21447600]

Fini ME, Bartlett JD, Matsubara M, Rinehart WB, Mody MK, Girard MT, Rainville M. The rabbit gene for 92-kDa matrix metalloproteinase. Role of AP1 and AP2 in cell type-specific transcription. J Biol Chem. 1994; 269:28620–28628. [PubMed: 7961810]

Fini, ME.; Cook, JR.; Mohan, R.; Brinckerhoff, CE. Regulation of matrixmetalloproteinase gene expression.. In: Parks, WC.; Mecham, RP., editors. Matrix metalloproteinases. Academic Press; p. 299-356.

Fini ME, Girard MT, Matsubara M, Bartlett JD. Unique regulation of the matrix metalloproteinase, gelatinase B. Invest Ophthalmol Vis Sci. 1995; 36:622–633. [PubMed: 7890493]

Gallus GN, Cardaioli E, Rufa A, Da Pozzo P, Bianchi S, D'Eramo C, Collura M, Tumino M, Pavone L, Federico A. Alu-element insertion in an OPA1 intron sequence associated with autosomal dominant optic atrophy. Mol Vis. 2010; 16:178–183. [PubMed: 20157369]

Hernandez MR. The optic nerve head in glaucoma: role of astrocytes in tissue remodeling. Prog Retin Eye Res. 2013; 19:297–321. [PubMed: 10749379]

Hollander DA, Barricks ME, Duncan JL, Irvine AR. Macular schisis detachment associated with angle-closure glaucoma. Arch Ophthalmol. 2005; 123:270–272. [PubMed: 15710832]

Honkanen RA, Jampol LM, Fingert JH, Moore MD, Taylor CM, Stone EM, Alward WLM. Familial cavitary optic disk anomalies: clinical features of a large family with examples of progressive optic nerve head cupping. Am J Ophthalmol. 2007; 143:788–794. [PubMed: 17362864]

Howell GR, Walton DO, King BL, Libby RT, John SWM. Datgan, a reusable software system for facile interrogation and visualization of complex transcription profiling data. BMC Genomics. 2011; 12:429. [PubMed: 21864367]

Huopaniemi L, Tyynismaa H, Rantala A, Rosenberg T, Alitalo T. Characterization of two unusual RS1 gene deletions segregating in Danish retinoschisis families. Hum Mutat. 2000; 16:307–314. [PubMed: 11013441]

Jenuwein T, Allis CD. Translating the histone code. Science. 2001; 293:1074–1080. [PubMed: 11498575]

Kahook MY, Noecker RJ, Ishikawa H, Wollstein G, Kagemann L, Wojtkowski M, Duker JS, Srinivasan VJ, Fujimoto JG, Schuman JS. Peripapillary schisis in glaucoma patients with narrow angles and increased intraocular pressure. Am J Ophthalmol. 2007; 143:697–699. [PubMed: 17386284]

Kawase K, Allingham RR, Meguro A, Mizuki N, Roos B, Solivan-Timpe FM, Robin AL, Ritch R, Fingert JH. Confirmation of TBK1 duplication in normal tension glaucoma. Exp Eye Res. 2012; 96:178–180. [PubMed: 22306015]

Kheradmand F, Werner E, Tremble P, Symons M, Werb Z. Role of Rac1 and oxygen radicals in collagenase-1 expression induced by cell shape change. Science. 1998; 280:898–902. [PubMed: 9572733]

Kleinjan DA, Bancewicz RM, Gautier P, Dahm R, Schonthaler HB, Damante G, Seawright A, Hever AM, Yeyati PL, van Heyningen V. Subfunctionalization of duplicated zebrafish pax6 genes by cis-regulatory divergence. PLoS Genet. 2008; 4(2):e29. others. [PubMed: 18282108]

Krivoy D, Gentile R, Liebmann JM, Stegman Z, Rosen R, Walsh JB, Ritch R. Imaging congenital optic disc pits and associated maculopathy using optical coherence tomography. Arch Ophthalmol. 1996; 114:165–170. [PubMed: 8573019]

Kuchtey J, Olson LM, Rinkoski T, Mackay EO, Iverson TM, Gelatt KN, Haines JL, Kuchtey RW. Mapping of the disease locus and identification of ADAMTS10 as a candidate gene in a canine model of primary open angle glaucoma. PLoS Genet. 2011; 7:e1001306. [PubMed: 21379321]

Li M, Sakaguchi DS. Expression patterns of focal adhesion associated proteins in the developing retina. Dev Dyn. 2002; 225:544–553. [PubMed: 12454930]

Lincoff H, Schiff W, Krivoy D, Ritch R. Optic coherence tomography of optic disk pit maculopathy. Am J Ophthalmol. 1996; 122:264–266. [PubMed: 8694098]

Lincoff H, Yannuzzi L, Singerman L, Kreissig I, Fisher Y. Improvement in visual function after displacement of the retinal elevations emanating from optic pits. Arch Ophthalmol. 1993; 111:1071–1079. [PubMed: 8352690]

Mackay DS, Henderson RH, Sergouniotis PI, Li Z, Moradi P, Holder GE, Waseem N, Bhattacharya SS, Aldahmesh MA, Alkuraya FS, Meyer B, Webster AR, et al. Novel mutations in MERTK associated with childhood onset rod-cone dystrophy. Mol Vis. 2010; 16:369–377. [PubMed: 20300561]

Moore M, Salles D, Jampol LM. Progressive optic nerve cupping and neural rim decrease in a patient with bilateral autosomal dominant optic nerve colobomas. Am J Ophthalmol. 2000; 129:517–520. [PubMed: 10764862]

Ochi H, Tamai T, Nagano H, Kawaguchi A, Sudou N, Ogino H. Evolution of a tissue-specific silencer underlies divergence in the expression of pax2 and pax8 paralogues. Nat Commun. 2012; 3:848. [PubMed: 22617288]

O'Leary BM, Davis SG, Smith MF, Brown B, Kemp MB, Almabrazi H, Grundstad JA, Burns T, Leontiev V, Andorf J, Clark AF, Sheffield VC, et al. Transcript annotation prioritization and screening system (TrAPSS) for mutation screening. J Bioinform Comput Biol. 2007; 5:1155–1172. [PubMed: 18172923]

Postel EA, Pulido JS, McNamara JA, Johnson MW. The etiology and treatment of macular detachment associated with optic nerve pits and related anomalies. Trans Am Ophthalmol Soc. 1998; 96:73–88. – discussion 88–93. [PubMed: 10360283]

Quigley HA, Broman AT. The number of people with glaucoma worldwide in 2010 and 2020. Br J Ophthalmol. 2006; 90:262–267. [PubMed: 16488940]

Ritch R, Darbro BW, Menon G, Khanna CL, Solivan-Timpe F, Roos BR, Sarfarazi M, Kawase K, Yamamoto T, Robin AL, Lotery AJ, Fingert JH. *TBK1* gene duplication and normal-tension glaucoma. JAMA ophthalmology. in press.

Roberts MD, Grau V, Grimm J, Reynaud J, Bellezza AJ, Burgoyne CF, Downs JC. Remodeling of the connective tissue microarchitecture of the lamina cribrosa in early experimental glaucoma. Invest Ophthalmol Vis Sci. 2009; 50:681–690. [PubMed: 18806292]

Roodhooft JMJ. Leading causes of blindness worldwide. Bull Soc Belge Ophtalmol. 2002:19–25. [PubMed: 12058483]

Rosenbloom KR, Dreszar TR, Long JC, Malladi VS, Slaon CA, Raney BJ, Cline MS, Karolchik D, Barber GP, Clawson H. ENCODE whole-genome data in the UCSC Genome Browser: update 2012. Nucleic Acids Res. 2012; 40(Database issue):D912–D917. others. [PubMed: 22075998]

Sanyal A, Lajoie BR, Jain G, Dekker J. The long-range interaction landscape of gene promoters. Nature. 2012; 489(7414):109–113. [PubMed: 22955621]

Savell J, Cook JR. Optic nerve colobomas of autosomal-dominant heredity. Arch Ophthalmol. 1976; 94:395–400. [PubMed: 945057]

Schiaffino MV, Bassi MT, Galli L, Renieri A, Bruttini M, De Nigris F, Bergen AA, Charles SJ, Yates JR, Meindl A. Analysis of the OA1 gene reveals mutations in only one-third of patients with X-linked ocular albinism. Hum Mol Genet. 1995; 4:2319–2325. [PubMed: 8634705]

Sivak JM, Fini ME. MMPs in the eye: emerging roles for matrix metalloproteinases in ocular physiology. Prog Retin Eye Res. 2002; 21:1–14. [PubMed: 11906808]

Slusher MM, Weaver RG, Greven CM, Mundorf TK, Cashwell LF. The spectrum of cavitary optic disc anomalies in a family. Ophthalmology. 1989; 96:342–347. [PubMed: 2710526]

Spaide RF, Costa DL, Huang SJ. Macular schisis in a patient without an optic disk pit optical coherence tomographic findings. Retina (Philadelphia, Pa.). 2003; 23:238–240.

Sternlicht MD, Werb Z. How matrix metalloproteinases regulate cell behavior. Annu. Rev. Cell Dev. Biol. 2001; 17:463–516. [PubMed: 11687497]

Tucker BA, Scheetz TE, Mullins RF, DeLuca AP, Hoffmann JM, Johnston RM, Jacobson SG, Sheffield VC, Stone EM. Exome sequencing and analysis of induced pluripotent stem cells identify the cilia-related gene male germ cell-associated kinase (MAK) as a cause of retinitis pigmentosa. Proceedings of the National Academy of Sciences. 2011; 108:E569–76.

Wang I-J, Chiang T-H, Shih Y-F, Lu S-C, Lin LL-K, Shieh J-W, Wang T-H, Samples JR, Hung P-T. The association of single nucleotide polymorphisms in the MMP-9 genes with susceptibility to

acute primary angle closure glaucoma in Taiwanese patients. Mol Vis. 2006; 12:1223–1232. [PubMed: 17110919]

Zumbro DS, Jampol LM, Folk JC, Olivier MMG, Anderson-Nelson S. Macular schisis and detachment associated with presumed acquired enlarged optic nerve head cups. Am J Ophthalmol. 2007; 144:70–74. [PubMed: 17493573]

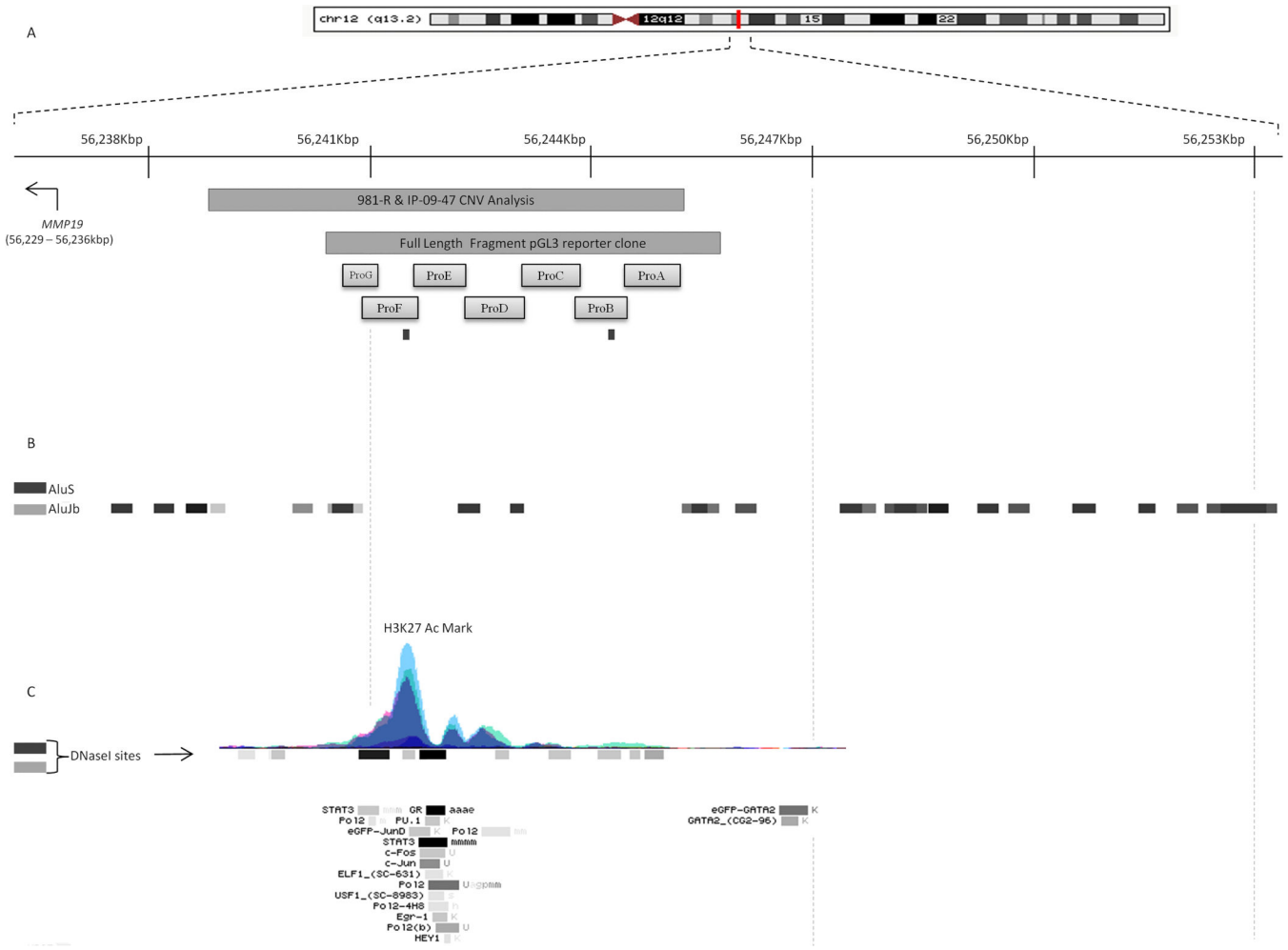

Figure 1. Chromosome 12 triplication upstream of *MMP19* gene

A. This schematic shows the results of the CNV analysis of the 981-R and IP-09-47 CODA pedigrees. A heterozygous triplication (2 extra copies) of a 6 Kbp DNA segment of chromosome 12q14 was detected upstream of the *MMP19* gene in members of pedigrees 981-R and IP-09-47 with CODA. The extent of the triplication in members of pedigrees IP-09-47 and 981-R is represented with a grey box labeled “981-R & IP-09-47 CNV Analysis” and the location of the transcription start site of the *MMP19* gene is indicated with a bent arrow. The portion of the 6 Kbp DNA segment that was used in the luciferase reporter assay is indicated with the grey box labeled “Full Length Fragment pGL3 reporter clone”. The segments of the CNV that were subcloned to assess for transcription activity are indicated by boxes labeled ProA – ProG. The location of the TaqMan qPCR probes used to assess copy number is shown below promoter fragments (black bars). **B.** The locations of Alu-repeat domains flanking the triplicated sequence are indicated with black or grey boxes which represent AluS and AluJb subtypes respectively. **C.** The triplicated sequence coincides with a region of H3K27 acetylation sites (indicated by the peaks above the horizontal line) and DNAseI hypersensitivity sites indicated by boxes below the horizontal line. Potential transcription factor binding sites identified by the UCSC browser are shown below the horizontal line.

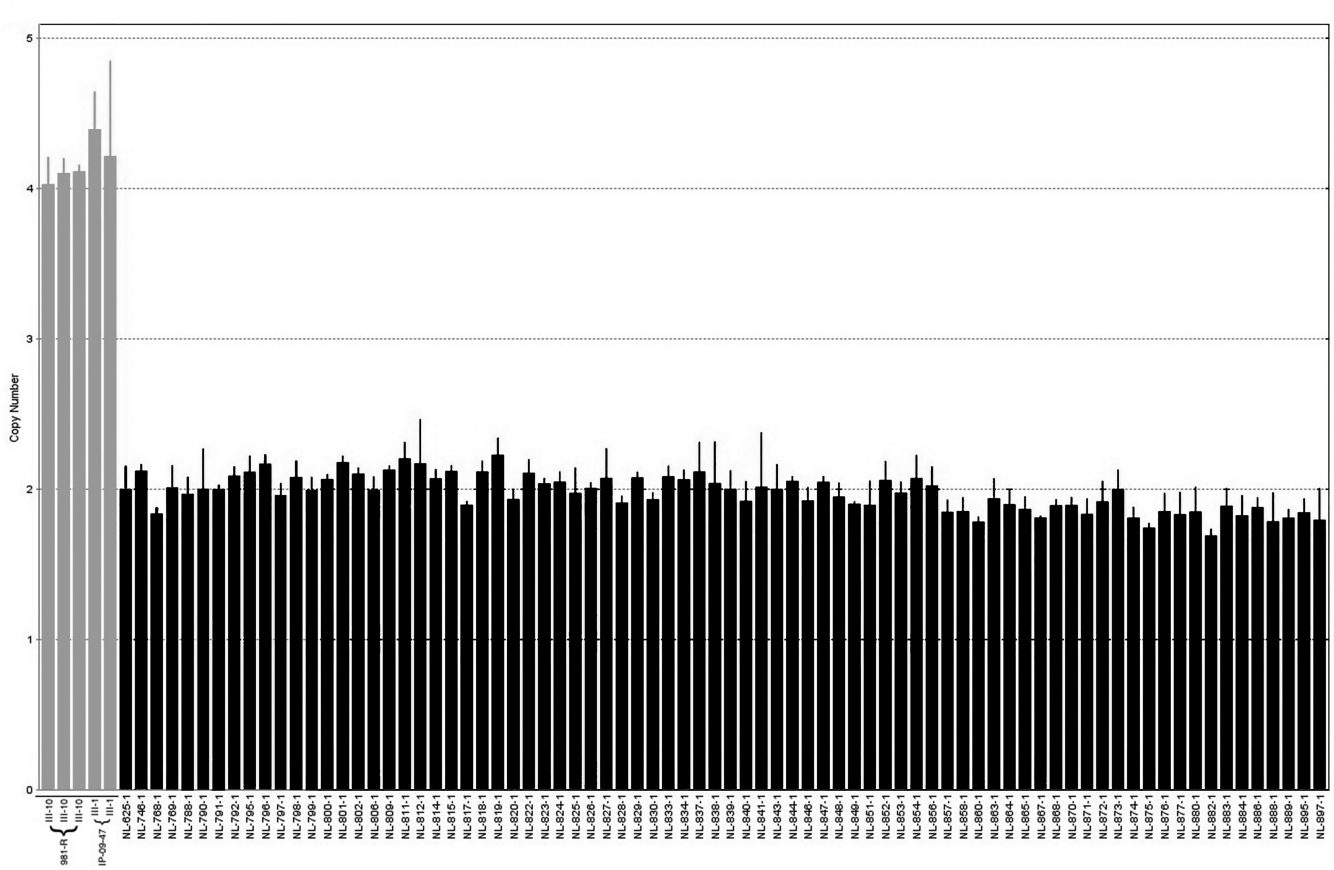

Figure 2. Quantitative PCR assay for chromosome 12q14 CNV

A TaqMan qPCR assay was used to test 24 unrelated CODA patients for the chromosome 12q14 triplication upstream of *MMP19*. A triplication was detected in one of these subjects, a member of pedigree IP-09-47. The results of testing members of CODA pedigrees 981-R and IP-09-47 and 78 control subjects with the qPCR assay are shown above.

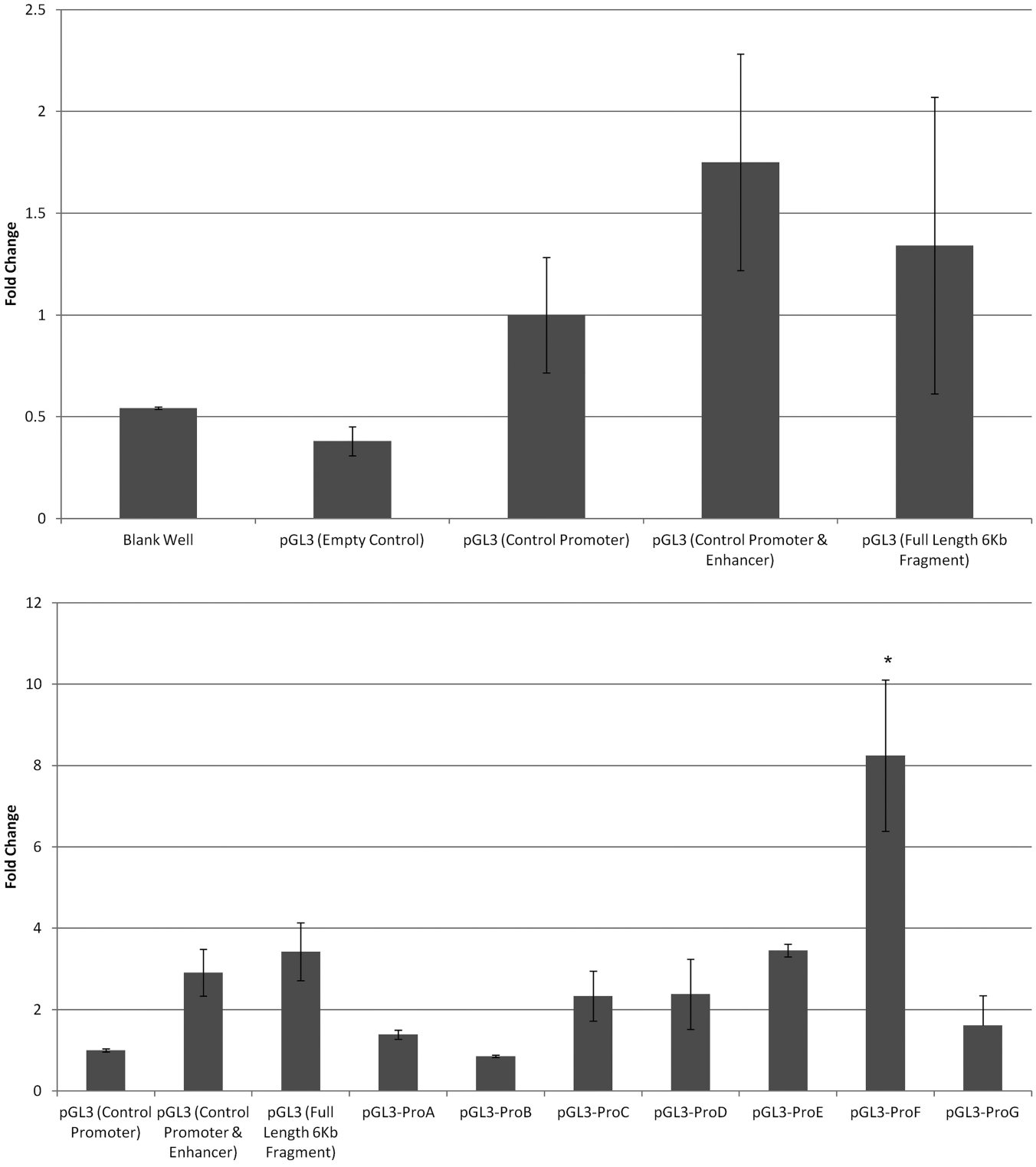

Figure 3. Triplicated *MMP19* promoter sequence has strong enhancer activity

A. Testing the 6 Kbp DNA segment spanned by the CNV for enhancer activity with a Luciferase reporter gene assay indicated this segment of DNA increased transcription by to 1.3-fold. **B.** Seven overlapping subclones that span the *MMP19* promoter CNV (ProA –

ProG) were tested for enhancer activity with the same Luciferase reporter gene assay. ProF increases transcription 8-fold ($p < 0.05$). All experiments were done in triplicate.

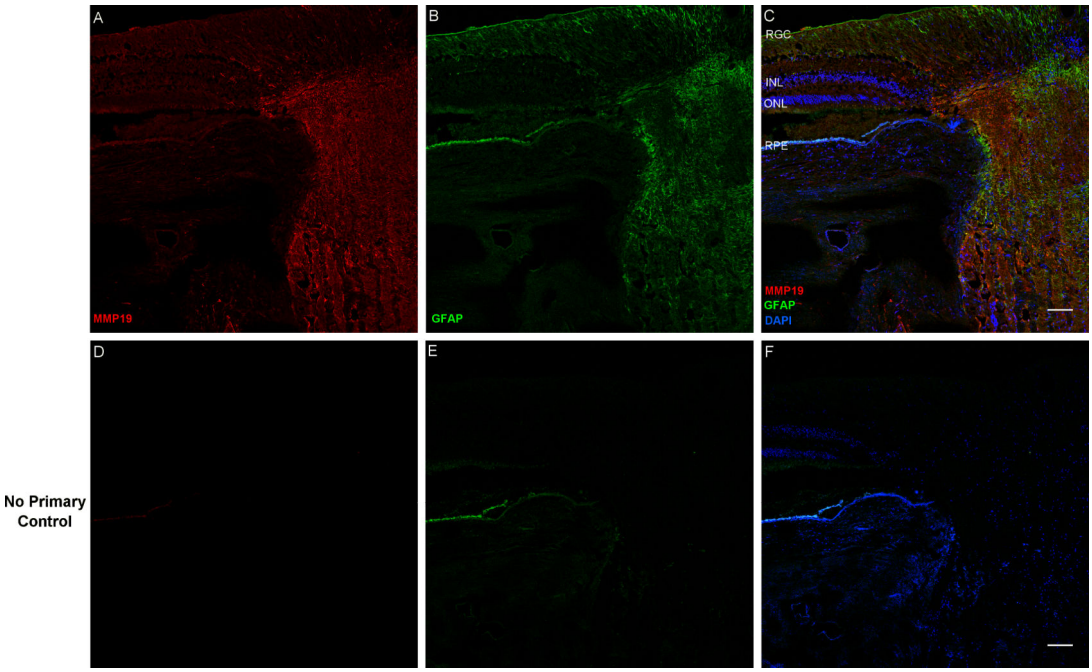

Figure 4. MMP19 is localized in the human optic nerve head

Immunolabeling of sagittal sections of a human donor eye shows that MMP19 is specifically expressed in the optic nerve head as well as the prelaminar and postlaminar optic nerve. **A-C.** MMP19 antibody only, GFAP antibody only, and merged image of MMP19, GFAP, and DAPI respectively. **D-F.** No primary control images of A-C. Experiments were done in triplicate and compared to immunolabeling with astrocyte marker GFAP. RGC = retinal ganglion cell, INL = inner nuclear layer, ONL = outer nuclear layer, RPE = retinal pigmented epithelium, ON = optic nerve. Scale bar = 100μm.

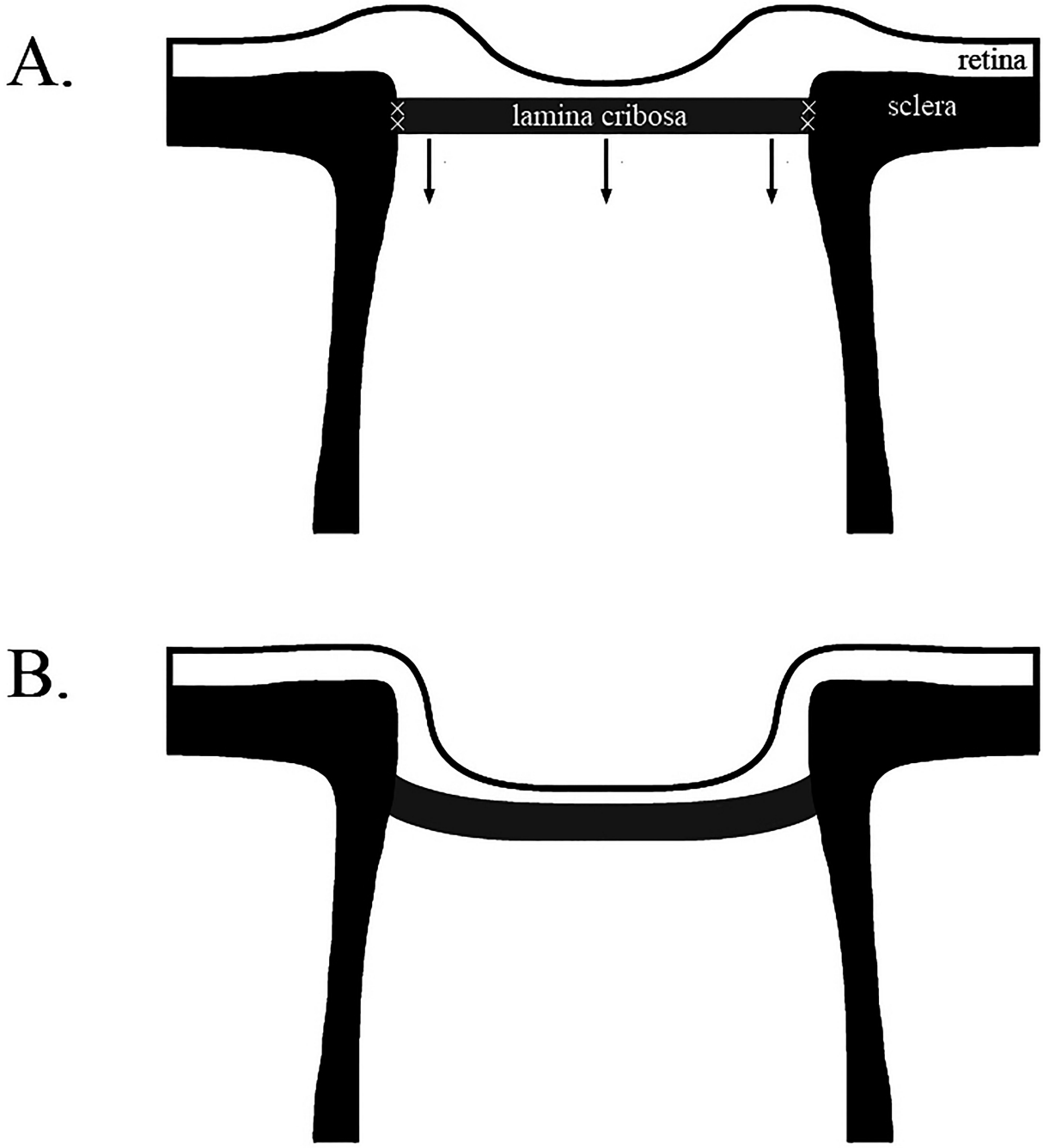

Figure 5. Model of MMP19 expression and optic disc excavation

The location of the retina, the sclera, and the lamina cribosa (support structure of the optic nerve) are shown in a cross-section of the eye that depicts moderate excavation of the optic disc (A). We hypothesize that MMP19 expression in the optic nerve, especially at the insertion of the lamina cribosa into the sclera (indicated by “X's”) may lead to collapse of the lamina cribosa and deepening of the optic nerve cup (B) that is seen in CODA. A similar process may be at work in glaucoma as well.